

Chapter 11

SOLAR RADIO EMISSION

W. R. Barron
E. W. Cliver
J. P. Cronin
D. A. Guidice

Since the first detection of solar radio noise in 1942, radio observations of the sun have contributed significantly to our evolving understanding of solar structure and processes. The now classic texts of Zheleznyakov [1964] and Kundu [1965] summarized the first two decades of solar radio observations. Recent monographs have been presented by Kruger [1979] and Kundu and Gergely [1980].

In Chapter I the basic phenomenological aspects of the sun, its active regions, and solar flares are presented. This chapter will focus on the three components of solar radio emission: the basic (or minimum) component, the slowly varying component from active regions, and the transient component from flare bursts.

Different regions of the sun are observed at different wavelengths. At millimeter wavelengths, the radiation is from the photosphere. Centimeter wavelength radiation originates in the chromosphere and low corona. Decimeter and meter wavelengths have their origin at increasing heights in the corona; at meter wavelengths the observed radiation comes from heights ranging from 100 000 to 700 000 km above the photosphere. For receiving equipment on the earth, the low-frequency limit for observation is the frequency at which radio waves are reflected by the ionosphere (for practical purposes, around 20 MHz). The high-frequency limit is set by absorption of radiation by atmospheric oxygen and water vapor. Recently, radio experiments on satellites have observed hectometric wavelength (≤ 2 MHz) emission that originate at heights ≥ 10 solar radii (R_{\odot}). This leaves only the frequency range from 2 to 20 MHz, corresponding to emission heights of 2–10 R_{\odot} , unexplored by radio methods.

11.1 BASIC DEFINITIONS

If the sun radiated only, as a thermal source, the emitted energy density would vary with frequency and temperature according to Planck's radiation law. In the radio region, the Rayleigh-Jeans approximation for blackbody radiation is valid; the brightness, radiance per unit bandwidth, is

$$B_{\nu} = 2kT\nu^2c^{-2} = 2kT\lambda^{-2}. \quad (11.1)$$

If the frequency ν is in cycles per second, the wavelength λ in meters, the temperature T in degrees Kelvin, the velocity of light c in meters per second, and Boltzmann's constant k in joules per degree Kelvin, then B_{ν} is in $W m^{-2}Hz^{-1}sr^{-1}$. Values of temperatures T_b calculated from Equation (11.1) are referred to as *equivalent blackbody temperature* or as *brightness temperature* defined as the temperature of a blackbody that would produce the observed radiance at the specified frequency.

The radiant power received per unit area in a given frequency band is called the power flux density (irradiance per bandwidth) and is strictly defined as the integral of $B_{\nu}d\Omega_{\nu}$ between the limits ν and $\nu + \Delta\nu$, where Ω_{ν} is the solid angle subtended by the source. In solar radio astronomy the relationship used is

$$F_{\nu} = B_{\nu}\Omega_{\nu} = 2kT_d\Omega_{\nu}\lambda^{-2}, \quad (11.2)$$

where the apparent or disk temperature T_d is that temperature which a uniform source of the same angular size as the solar optical disk must have in order to produce the power flux density F_{ν} received from the sun. Values of power flux density are usually given in solar flux units (1 solar flux unit, sfu = $10^{-22} W m^{-2} Hz^{-1}$).

The power P_s received at the antenna due to solar radiation is given by:

$$P_s = F_{\nu}A_e, \quad (11.3)$$

where A_e is the effective area of the antenna. P_s is also conveniently expressed in terms of the effective antenna temperature T_A corrected for any RF losses. T_A is defined by

$$P_s = kT_A\Delta\nu. \quad (11.4)$$

T_A is readily measured with suitably calibrated instruments. The equation for calculating the solar power flux density

CHAPTER 11

from a given antenna temperature measured at a given installation is

$$F_s = 2kT_A \frac{L}{A_c}, \quad (11.5)$$

where A_c is the effective area of the antenna in square meters, and L is a dimensionless correction factor related to the antenna response shape and to the diameter and temperature distribution across the source. The value of L is unity only if the antenna half-power beamwidth is large compared to the source. L exceeds unity when the ratio of the antenna half-power beamwidth to the solar angular diameter drops below about five; thus, it is desirable to use a parabola small enough so the half-power beamwidth is more than five times the solar angular diameter. Once the solar flux density is known, the apparent temperature and the brightness of the solar disk may be calculated from Equation (11.2).

11.2 THE MINIMUM (ZERO-SUNSPOT) COMPONENT

The standard method for obtaining the basic radio flux density of the unspotted sun is to make a scatter plot of solar temperature at a given frequency against the projected sunspot area; the extrapolation of the curve that best fits these data to zero sunspot area determines the minimum or basic flux density at that frequency. By doing this for all frequencies, one determines the spectrum of the basic component of solar radiation. Figure 11-1 shows the distributions of power flux density for the sun and for black bodies at various temperatures. It is only at millimeter and shorter

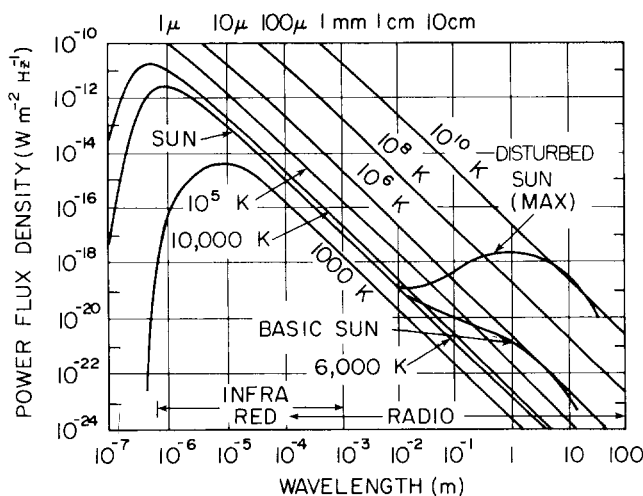


Figure 11-1. Solar spectrum and spectra of blackbody radiation at various temperatures. The solar power-flux density (power per unit area per unit bandwidth) is plotted against wavelength.

wavelengths that solar radio emission approximates a 6000 K blackbody. At wavelengths longer than 1 cm, the equivalent blackbody temperature ranges between 10^4 to 10^6 K for the spotless sun and from 10^4 to 10^{10} K for the disturbed sun depending on the condition of the sun and the time in relation to the 11-year sunspot cycle. Meter wavelengths are characterized by much burst activity; thus, the basic (or minimum) sun temperatures at these wavelengths are determined by making observations over a period of weeks or months. The low temperature to which the sun periodically returns, but never goes below, during this period is taken to be the zero-sunspot value; it is of the order of 10^6 K.

11.3 THE SLOWLY VARYING COMPONENT

The slowly varying component (SVC) exhibits a well defined 11-year cycle variation and a 27-day solar-rotation variation, since this emission originates principally in coronal condensations overlying active regions, and is well-correlated with sunspot number. The routine daily measurement of the combination of the basic (or minimum) component and the SVC of solar radio emission is referred to as the *quiet-sun flux density*. The SVC of the sun as a whole is obtained by subtracting the basic component from the quiet-sun flux density. The SVC of individual active regions can be obtained by either eclipse observations or interferometric measurements.

11.4 THE BURST COMPONENT

During solar flares (Chapter 1) there may be large increases (bursts) in radio emission lasting anywhere from a few seconds to several hours. These bursts originate by bremsstrahlung, gyrosynchrotron, and plasma radiations. Characteristics of the bursts vary with wavelength. Bursts in the meter-wave range (12 m to about 50 cm) are classified by spectral type. No spectral classification exists for the decimeter or centimeter wave regions.

11.4.1 Meter-Wave Range (25 – 500 MHz).

Most information on solar bursts in the range from 12 m to about 50 cm is obtained from swept-frequency observations. Dynamic spectra are displayed on a cathode-ray tube and recorded photographically as a series of intensity-modulated traces that give intensity as a brightening in the frequency-time plane. Figure 11-2 is an illustration of idealized dynamic spectra of various types of bursts. These spectral types are discussed below in the order of their occurrence in the flare event.

Type III bursts are the most common type of solar radio

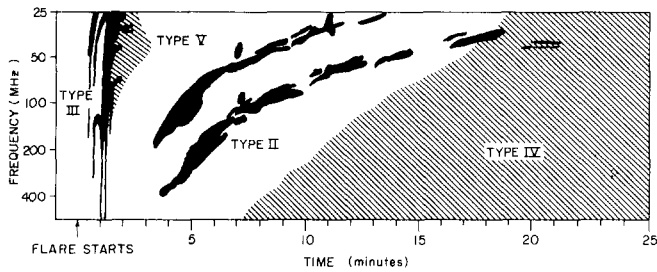


Figure 11-2. Idealized illustration of the record of a complete solar radio outburst as recorded by a dynamic spectrograph at meter wavelengths.

activity. They can occur either singly (duration ~ 5 s) or in groups. Only about one-third of Type III bursts are associated with flares. When associated with flares, however, the timing agreement with flare impulsive hard x-ray and microwave emission is often quite good (within seconds). Type III bursts are caused by streams of ~ 100 keV electrons propagating outward through the solar atmosphere and exciting plasma waves. Because of their relatively high drift rates (20 MHz/s) to lower frequencies, they are referred to as fast drift bursts.

Type V bursts consist of a broad band continuum of short duration (~ 1 min) that is preceded by a Type III burst and accompanied by centimeter-wave and hard x-ray bursts. The Type V burst may indicate the presence of a particularly rich stream of electrons, part of which is trapped in the corona and becomes visible either through gyrosynchrotron radiation or plasma waves.

The Type II burst, or slow-drift (~ 0.2 MHz/s) burst is presumed due to the presence of a shock wave propagating outward through the solar corona with a characteristic velocity of 1000 km/s. The disturbance excites plasma waves at the local plasma frequency. In the spectrograph record, these bursts appear as a narrow band of intense radiation that drifts gradually and often irregularly from high to low frequency. About 60% of all Type II bursts show emission at the second harmonic. Type II bursts are closely associated with solar flares.

Type IV emission has at least three distinct components; these components can not be separated on the spectrograph record and can only be distinguished by interferometers. *Flare continuum* is the broad band emission occurring at meter and decimeter wavelengths during the flare impulsive phase. *Moving Type IV* bursts involve a variety of forms, although three basic types have been recognized. These are the magnetic arch, the advancing front, and the isolated source (ejected plasma "blob"). Both the flare continuum and moving Type IV emissions have durations ≤ 10 –60 min. While the moving Type IV burst travels outward through the corona and can reach heights of $\sim 10^9$ km above the photosphere, the final stage of Type IV emission, the *storm continuum*, originates low in the corona near the corresponding plasma level and directly above the site of the

optical flare. The storm continuum can last for several hours and often degenerates into the Type I noise storms whose durations range from hours to days. In contrast to the flare continuum and moving Type IV emissions that are only weakly polarized, storm continuum is strongly polarized in the ordinary mode. This suggests plasma radiation as the source of the storm continuum, while gyrosynchrotron radiation from energetic electrons spiraling in weak coronal magnetic fields are generally cited as the source of the flare continuum and moving Type IV emissions.

Type I events are distinguished from the relatively smooth broad-band Type IV emission by the presence of a great number of short (~ 1 s) intense bursts superimposed on the background continuum. These short intense bursts are distributed more or less randomly over the frequency range of the underlying continuum. Both the background continuum and the superimposed bursts are strongly circularly polarized, usually in the ordinary mode. Type I radiation appears to be more closely associated with certain active regions than with flares, although they can be flare-initiated. At present, the mechanism and origin of Type I emission are not well understood.

11.4.2 Decimeter-Wave Range (500 – 2000 MHz).

At decimeter wavelengths the emission is highly variable and complex. Rapid time structures (several peaks per minute) are often observed in the time profiles of decimetric radio bursts observed at discrete frequencies, and the relationship of these fast structures to the source of the smoother emission observed at centimeter wavelengths is not clear. Individual peaks in complex events are often strongly circularly polarized in the ordinary mode.

11.4.3 Centimeter-Wave Range (2000 – 35000 MHz).

Solar emission in the 15–1 cm range does not show as rapid fluctuations as emission in the meter and decimeter ranges. There appear to be at least two basic morphological types of centimeter-wave bursts. The first of these is the *simple impulsive event* that reaches a maximum peak-flux density ranging from 10^1 to $>10^4$ sfu in a few minutes. Impulsive bursts are interpreted in terms of gyrosynchrotron emission. Complex bursts may consist of several impulsive events in sequence, although the appearance of a relatively smooth broad band microwave Type IV component in the later stages of many complex events may indicate an additional or prolonged acceleration process. The second of these, the *gradual rise and fall* microwave burst, may occur by itself or may follow an impulsive event (monotonic decay only), in which case it is referred to as a *post-burst* event.

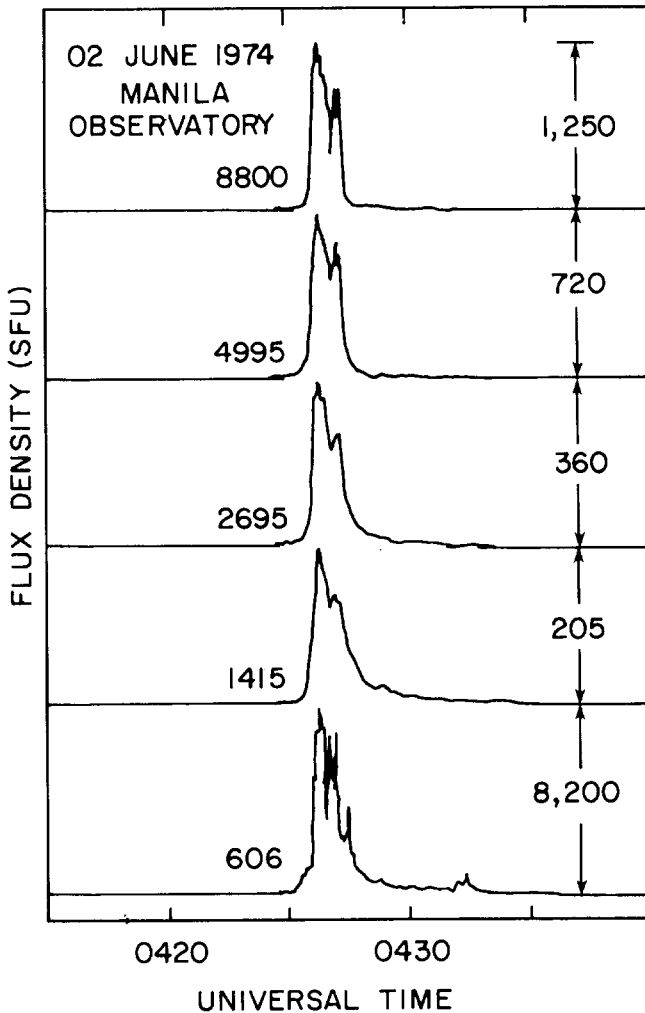


Figure 11-3. The time-intensity profile of an impulsive microwave burst.

Peak flux densities of these gradual events seldom exceed 50 sfu; these events are generally explained in terms of bremsstrahlung from a Maxwellian distribution of electrons. Examples of the time profiles of microwave bursts observed at Sagamore Hill Solar Radio Observatory are contained in the burst atlas compiled by Barron et al. [1980]. A typical impulsive event is presented in Figure 11-3.

Instantaneous spectra of events in the centimeter frequency range are relatively smooth and tend not to have narrow-band emission features. For moderate sized events (≥ 100 sfu), the peak-flux-density spectral maximum of the emission generally occurs at frequencies ≥ 9 GHz. For the largest events with centimeter wave peak flux densities ≥ 1000 sfu, the emission usually extends to the meter-wave range where it often exhibits a second spectral maximum with a minimum occurring at the intermediate wavelengths. This U-shaped spectral signature (Figure 11-4) is thought to reflect the fact that there are two different sources of burst radiation (one at centimeter waves and one at lower fre-

quencies) with different electron energy distributions and different magnetic fields [Kundu and Vlahos, 1982].

11.5 CORRECTIONS TO QUIET-SUN AND BURST-FLUX DENSITIES

In the final two sections of this chapter, charts and tables of burst and quiet-sun flux densities from Sagamore Hill Solar Radio Observatory are presented. It is appropriate to discuss errors of absolute calibrations in these measurements. In 1973, a report [Tanaka et al., 1973] by an absolute calibration working group formed by Commission V of URSI was published. It contained corrections for Sagamore Hill for the years 1966–1971. For the years 1972–1976, correction factors were taken from the IAU's *Quarterly Bulletin of Solar Activity*. For 1977–1979, correction factors were derived by extrapolation from previous years and comparison of the Sagamore Hill quiet-sun flux densities with those of other solar-patrol observatories. For 245 MHz, a substantial correction factor (1.55) was applied to all the data as a result of an absolute calibrations measurement (using the radio source Cassiopeia A) carried out at Sagamore Hill in 1980. The multiplicative flux-density correction factors for the five frequencies for which data are presented are listed in Table 11-1. Before processing the data presented below, these correction factors were applied to the Sagamore Hill burst and quiet-sun data.

11.6 QUIET-SUN FLUX-DENSITY MEASUREMENTS

Solar microwave emission correlates well with solar EUV flux [Forbes and Straka, 1973], a fact which makes it useful as an input to ionospheric models in lieu of the more difficult to obtain sunspot number and EUV flux. For this reason, the 1965 edition of the *Handbook of Geophysics* included a table of the daily quiet-sun (non-bursting) flux densities observed at 2800 MHz (10.7 cm wavelength) by the National Research Council in Ottawa, Canada from 1947 to mid-1963. We continue the table in this handbook using Ottawa data through 1965 and Sagamore Hill data thereafter. In addition, the 8800 MHz quiet-sun flux-density values from Sagamore Hill are included.

In Table 11-2 we present the observed daily solar flux density value measured at 2800 MHz at Ottawa for the years 1963–1965 and the 2695 and 8800 MHz flux density values measured at the Sagamore Hill Radio Observatory from January 1966 through December 1979. It should be noted that these are observed values and not values adjusted to 1 AU. The values are taken at local noon at the Sagamore Hill meridian. This is done so that the radiation will have passed through the shortest path in the earth's atmosphere

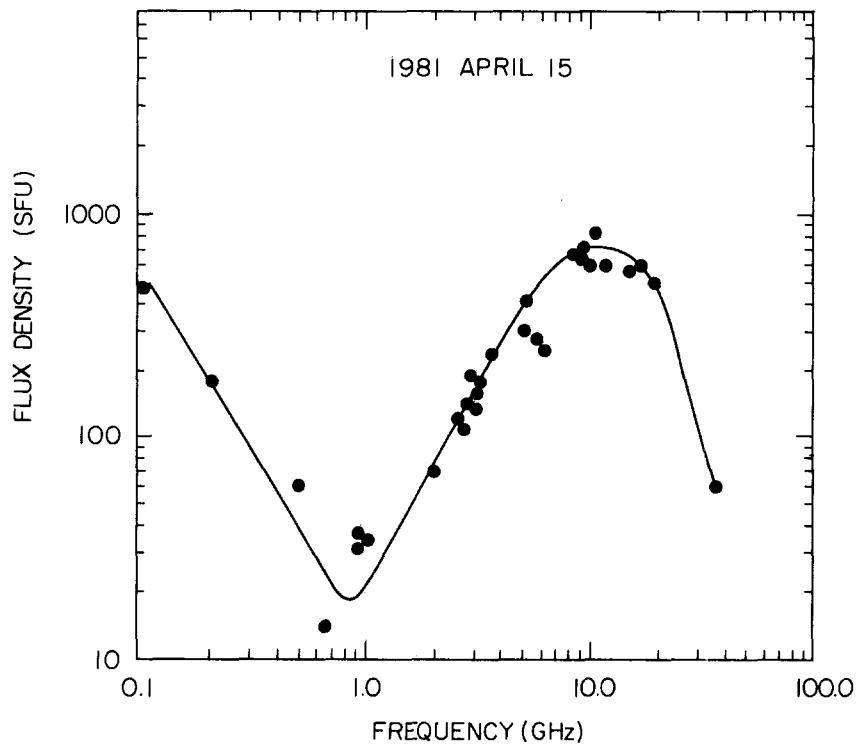


Figure 11-4. The peak flux-density spectrum of a large microwave burst. The U-shape is characteristic for large microwave bursts with peak flux density > 1000 sfu.

and be subject to the minimum atmospheric attenuation. In some instances this meridian-transit observation is not possible because a solar radio burst is in progress at that time. When this happens, the observation is taken as soon as it has been determined that the radio burst has ended. In virtually all cases this was within an hour of the time of meridian transit so that the added attenuation due to the increased atmospheric path length was negligible.

Note the asterisk (*) between the 2695 MHz flux-density value and the 8800 MHz flux-density value on some days. This indicates that there were adverse weather conditions, usually rain or snow, present when the observations were being made. These conditions will cause the signals received to be further attenuated. The asterisk indicates that some adjustment has been made to the observed value to compensate for this problem.

Table 11-1. Calibration correction factors, Sagamore Hill, 1966-1979.

Year	245 MHz	610 MHz	1415 MHz	2695 MHz	8800 MHz
1966	—	0.91	1.16	0.90	0.91
1967	—	0.91	1.16	0.90	0.91
1968	—	0.91	1.16	0.90	0.95
1969	1.55	0.91	1.16	0.94	1.00
1970	1.55	0.91	1.16	0.94	1.00(2)
1971	1.55	0.91	1.16	0.94	1.00(2)
1972	1.55	0.91	1.08	0.93	0.95
1973	1.55	0.91	1.03	0.91	0.90
1974	1.55	0.91	1.05	0.90	0.90
1975	1.55	0.91	1.05	0.90	0.87
1976	1.55	0.92	1.08	0.90	0.85
1977	1.55	1.00	1.06	0.88	0.88
1978	1.55	1.00	1.06	0.85	0.87
1979	1.55	1.00	1.06	0.85	0.84

Notes: (1) For the period 9 June to 31 August 1967, all 2695 MHz burst and daily flux-density values should be multiplied by 1.13.
 (2) For the period 1 November 1970 to 31 August 1971, all 8800 MHz burst and daily flux-density values should be multiplied by 1.14.

CHAPTER 11

11.7 SOLAR RADIO-BURST CLIMATOLOGY BASED ON 1966-1978 SAGAMORE HILL OBSERVATIONS

In addition to its role in maintaining the ionosphere, the sun is the most powerful natural source of radio interference to ground-based or near-earth (aircraft or satellite) radio receivers. Therefore, it is of interest to designers and operators of radio receiving equipment to have information on what sort of interference one might expect from the sun at different frequency ranges in the radio spectrum and over what percentage of time the interference might occur (above a certain intensity level). Since radio burst emission from the sun varies unpredictably over a wide range of frequencies, one can only give the statistical likelihood of certain levels being exceeded at various frequencies (or frequency ranges) of interest. We call this body of statistics on solar radio-burst occurrence "climatology." Burst climatology is provided by Sagamore Hill observations at 245, 610, 1415, 2695, and 8800 MHz [Castelli et al., 1973]. Observations at 245 MHz began in March 1969; observations for the other listed frequencies began in January 1966.

To produce a useful solar-burst "climatology", one must first determine what intensity (flux-density) level a burst must reach to interfere with operational systems. Since radio-burst emission occurs over only a very small fraction of the time that any system is exposed to the sun's steady-state (quiet-sun) radio emission, the "disruptive" level of burst emission must be significantly greater than the quiet-sun flux-density levels which vary over the 11-year solar-activity cycle (Figure 11-5).

Since the quiet-sun flux densities are different at different frequencies, one could choose a burst level greatly exceeding the quiet-sun level at any frequency covered in the climatology study (1000 sfu, for example). One could also choose a burst level at each frequency that is a fixed multiple of the mean monthly quiet-sun emission (for ex-

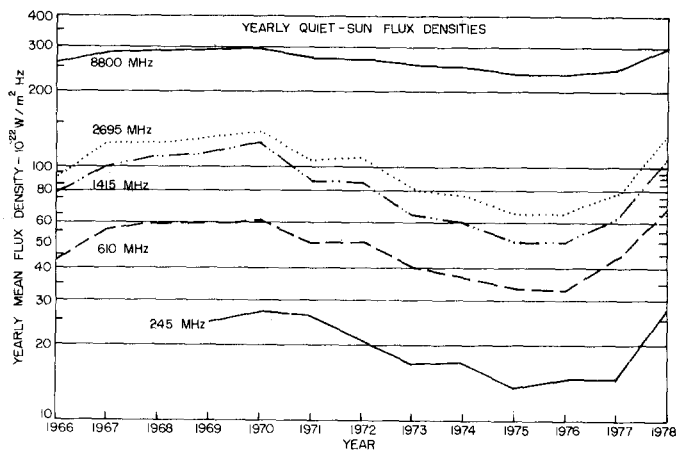


Figure 11-5. Yearly quiet-sun flux densities for several frequencies measured at Sagamore Hill.

Table 11-2a. Daily values of observed solar flux density at 2800 MHz recorded at the Algonquin Radio Observatory (ARO) of the National Research Council, Ottawa, Canada.

DAY	1963											
	JAN	FEB	MAR	APR	MAY	JUN	JUL	AUG	SEP	OCT	NOV	DEC
01		87	74	73	82	84	76	87	74	68	87	79
02		86	75	74	82	81	77	87	73	69	85	80
03	77	85	78	74	81	81	78	87	74	70	83	79
04	79	88	80	70	82	79	78	88	75	71	83	77
05	77	87	82	72	84	78	78	86	74	73	80	76
06	77	85	85	78	87	77	77	88	74	77	78	76
07	77	83	84	80	88	84	77	85	78	79	76	77
08	76	82	83	81	86	90	77	81	75	85	75	77
09	78	79	82	82	88	83	77	86	77	86	76	78
10	80	79	80	82	87	99	86	77	99	87	75	79
11	81	76	78	88	84	103	75	72	72	87	76	80
12	78	74	77	93	87	109	74	73	77	84	77	82
13	79	74	74	89	89	107	76	74	89	84	77	81
14	86	75	80	87	95	100	77	71	98	96	78	79
15	85	76	80	88	98	96	76	72	99	88	81	81
16	82	77	79	88	100	89	76	76	105	87	81	78
17	82	79	79	87	100	86	74	82	99	84	80	78
18	80	81	80	88	98	82	74	80	97	83	82	79
19	78	79	77	84	99	79	74	79	102	88	86	78
20	78	77	77	78	91	75	77	81	109	89	84	79
21	76	74	76	74	88	73	75	84	90	94	86	79
22	75	75	76	72	89	72	73	86	105	96	86	77
23	74	75	75	71	93	72	72	90	99	94	84	76
24	73	76	75	73	89	72	72	87	95	94	83	76
25	74	78	75	72	83	74	74	85	86	96	82	76
26	73	77	73	72	76	74	73	82	84	96	82	74
27	81	75	74	75	90	72	74	80	78	88	81	74
28	80	74	73	78	79	74	73	77	74	84	79	73
29	79	75	75	78	80	73	77	77	71	85	79	72
30	78	74	80	83	76	84	77	69	85	79	71	71
31	82	71	71	89	89	85	77	82	82	82	71	71
MEAN	78	79	78	79	88	83	76	81	85	84	81	77
DAY	1964											
	JAN	FEB	MAR	APR	MAY	JUN	JUL	AUG	SEP	OCT	NOV	DEC
01		73	78	77	69	68	67	67	70	72	75	76
02	71	72	75	75	68	68	67	68	69	72	74	76
03	73	71	74	77	70	68	67	68	70	72	74	77
04	75	71	75	77	70	68	68	68	70	71	73	78
05	74	72	72	76	72	68	68	69	70	72	73	78
06	75	75	74	76	71	68	68	68	70	73	74	77
07	75	72	73	76	71	68	68	68	71	73	75	76
08	73	73	74	74	72	70	67	68	71	77	72	77
09	73	72	72	75	71	69	67	68	71	73	72	77
10	73	73	73	73	70	70	67	69	72	73	72	78
11	75	72	75	74	70	70	68	68	72	72	72	80
12	76	73	77	73	79	69	67	70	72	70	72	77
13	76	73	78	73	68	70	66	74	72	72	72	78
14	76	73	79	72	68	70	69	76	72	71	73	78
15	75	73	79	71	68	72	70	75	71	71	72	78
16	74	73	77	71	70	71	69	73	70	71	72	80
17	72	74	78	72	70	71	69	72	68	71	76	80
18	74	76	75	72	70	72	68	70	68	72	75	80
19	75	76	74	71	69	70	67	71	69	73	75	81
20	76	76	74	71	68	70	67	70	69	73	76	80
21	75	78	74	72	68	70	66	69	69	71	74	78
22	75	80	78	71	67	70	66	69	69	72	73	78
23	75	84	77	70	67	67	66	69	68	73	72	76
24	74	85	77	72	68	68	66	68	68	74	71	75
25	73	84	74	71	68	68	66	68	68	76	71	75
26	74	86	74	70	68	68	65	68	69	76	70	74
27	73	85	75	70	68	67	65	68	70	76	72	76
28	77	84	76	70	70	67	65	67	70	74	71	77
29	78	81	75	69	69	67	66	67	71	74	73	78
30	75	78	78	69	68	67	66	69	71	74	74	77
31	74	77	77	68	68	67	66	69	71	74	74	77
MEAN	74	76	76	72	69	69	67	69	70	73	73	78
DAY	1965											
	JAN	FEB	MAR	APR	MAY	JUN	JUL	AUG	SEP	OCT	NOV	DEC
01	86	78	76	71	71	71	76	72	75	92	79	75
02	84	79	75	72	71	74	76	75	76	93	80	75
03	82	79	75	71	71	75	76	77	77	96	81	75
04	81	77	75	71	70	78	76	78	77	98	80	74
05	80	76	76	71	69	78	75	76	79	92	78	75
06	80	76	77	71	70	78	78	79	77	85	81	76
07	78	77	77	71	71	77	82	80	78	84	85	75
08	78	75	74	70	72	78	81	77	79	83	80	77
09	77	75	73	72	72	79	81	78	76	83	82	75
10	76	76	73	73	72	78	80	76	76	80	84	75
11	75	74	72	74	71	76	80	77	76	76	84	76
12	75	73	74	73	72	76	78	76	75	75	81	76
13	75	72	76	74	74	77	76	75	75	76	77	74
14	74	72	75	75	75	76	75	74	75	76	75	75
15	75	73	73	75	80	77	74	73	75	74	76	77
16	74	73	71	75	86	76	72	74	74	72	74	78
17	74	73	72	73	91	76	72	72	74	72	74	78
18	74	72	75	73	90	78	72	73	73	72	75	78
19	74	72	77	74	92	75	72	74	73	72	73	77
20	76	71	74	72	95	76	73	74	73	73	73	74
21	77	72	74	73	93	76	73	74	72	73	72	74
22	77	72	73	73	92	78	72	73	71	76	72	72
23	76	73	73	73	86	80	71	73	72	79	71	73
24	76	74	72	71	85	78	70	73	76	76	71	71
25	76	74	74	70	81	79	70	72	76	78	71	72
26	76	74	73	69	78	79	69	72	77	78	72	77
27	79	76	72	69	76	78	70	74	78	78	74	84
28	77	76	72	70	74	77	71	73	80	77	77	84
29	79	72	70	74	76	71	74	87	77	74	74	85
30	81	71	70	74	77	71	75	89	76	75	82	85
31	80	72	72	72	71	71	75	78	78	78	81	81
MEAN	78	75	74	72	78	77	74	75	76	80	77	76

CHAPTER 11

ample, five times the quiet-sun level). This climatology presents results using both approaches.

With regard to the statistics of burst levels over a certain threshold (flux-density level), one might want to know how many level-exceeding bursts occur in a given period (in a 24-hr day, for example). One might also like to know for what fraction of time (min per 24-hr day, for example) do bursts remain above a certain threshold. Again, both kinds of statistics are presented in this climatology.

The radio-burst climatology presented here is based on routine, daily, whole-sun patrol observations made at the Sagamore Hill Radio Observatory over the years 1966 to 1978. This period covers the decline from the maximum of the 20th solar cycle (a relatively low-amplitude cycle) through the minimum (around 1976) to the rising portion of the new (and higher-amplitude) 21st solar cycle. Data from the 1966–1978 period should provide a reasonable measure of the intensity/duration parameters of solar-burst radio emission during the least and most disturbed portions of the solar cycle.

The Sagamore Hill data on radio bursts, published routinely in *Solar Geophysical Data*(SGD) are given in terms of the following parameters: the peak flux density S_p (sfu), the mean flux density S_{me} (sfu) and the duration (min) T_d from start to end. These parameters are illustrated for the idealized burst in Figure 11-6. The area under the curve is

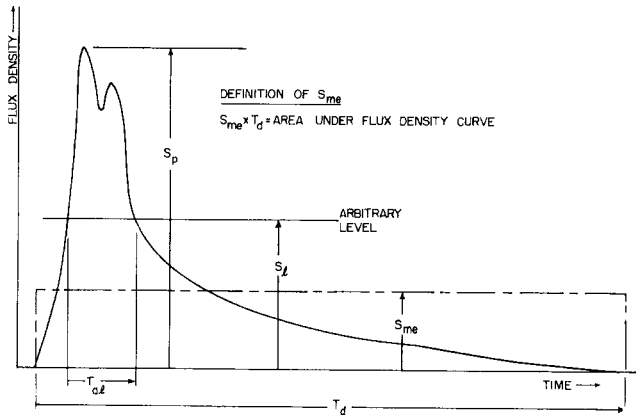


Figure 11-6. Burst parameters depicted for a typical microwave event. The symbols are explained in the text.

the time-integrated flux density. The mean flux density S_{me} is defined as the amplitude (flux density) of a rectangle with area equal to the time-integrated flux density and duration equal to the burst duration T_d .

In Figure 11-6, we have also shown an arbitrary flux density level, S_l . In the climatology study, we eventually want to derive (from the SGD-listed data alone) the time that bursts exceed a certain level. To illustrate the discussion that follows, we have shown the level S_l between S_p and S_{me} (if $S_l > S_p$, the burst would never exceed the arbitrary

level). We have also shown the “above-the-level” time, T_{al} .

For $S_{me} < S_l$, the longest possible length of time that a burst with mean flux density S_{me} could exceed the S_l threshold is $S_{me}/S_l \times T_d$. This is the worst case; it comes nowhere near representing the results for actual bursts.

In similar fashion if $S_{me} > S_l$, the longest possible length of level-exceeding time would be T_d . Obviously, this maximum result is not representative of T_{al} . A burst with an extremely large very-steep peak and long low-level tail could have its mean S_{me} greater than S_l , yet its flux density could lie below S_l for the overwhelming majority of the burst duration time T_d .

For each burst there is a factor by which $(S_{me}/S_l)T_d$ [for $S_{me} < S_l$] or T_d [for $S_{me} > S_l$] exceeds the actual “above-the-level” time T_{al} . We do not have the resources to go over the time profiles of every burst at each frequency. Therefore we had to look at a representative sample of bursts and derive an overall factor to multiply the $(S_{me}/S_l)T_d$ or T_d obtained from the SGD data.

Analysis of a limited number of relatively large events from a Burst Atlas compiled by Barron et al. [1980] shows that the factor by which $(S_{me}/S_l)T_d$ or T_d overstates T_{al} varies between 1.5 and 10, independent of frequency, with a mean of about 3. Therefore, we have used the following relationships to derive the “above the level” times of bursts from the flux-density and whole-burst duration data listed in *Solar Geophysical Data*:

$$T_{al} = \frac{1}{3}(S_{me}/S_l) T_d \text{ for } S_{me} < S_l \quad (11.6)$$

$$T_{al} = \frac{1}{3} T_d \quad \text{for } S_{me} > S_l.$$

Having discussed the data limitations and the approximating adjustments, we now present the results of the burst climatology study. In Figure 11-7, we show the number of bursts (statistically) per 24-hr day exceeding 500% of the quiet-sun (flux-density) level. The numbers are given for five frequencies (245 MHz, 610 MHz, 1415 MHz, 2695 MHz and 8800 MHz) over the years 1966 to 1978. In Figure 11-8 we show the number of bursts (statistically) per 24-hr day exceeding a flux-density level of $10^{-19} \text{ W/m}^2\text{Hz}$ (1000 sfu).

In Figure 11-9, we show the time duration (min per 24-hr day) that bursts exceed (statistically) 500% of the quiet-sun flux density level. These durations are given, as in the previous graphs, for the five patrol frequencies over the years 1966 to 1978. In Figure 11-10 we show the duration (min per 24-hr day) that bursts exceed (statistically) the $10^{-19} \text{ W m}^2 \text{ Hz}^{-1}$ flux-density level.

The burst number and duration statistics (in Figures 11-7 through 11-10) are given on a “per 24-hr day” basis. Obviously, the sun is not in view (available to provide

SOLAR RADIO EMISSION

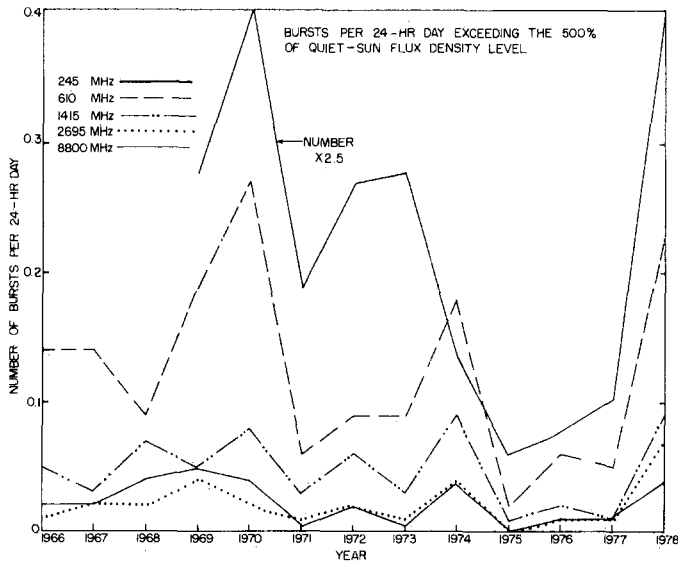


Figure 11-7. The number of bursts per day that exceeded 500% of the quiet-sun flux-density level for the years 1966–1978.

interference) 24 hours a day from any ground-based operating location. On sites far from the equator (high latitudes), sun-in-view hours per day vary widely with season. Also, the system susceptible to solar radio interference may be in operation only during certain hours of the day (or night). Hence, the best method of presentation is to give the statistics on a “per 24-hr day” basis and let the user determine what fraction of his operating time the sun is actually above the horizon to provide interference to his system. Finally, it is important to point out that the relatively low average

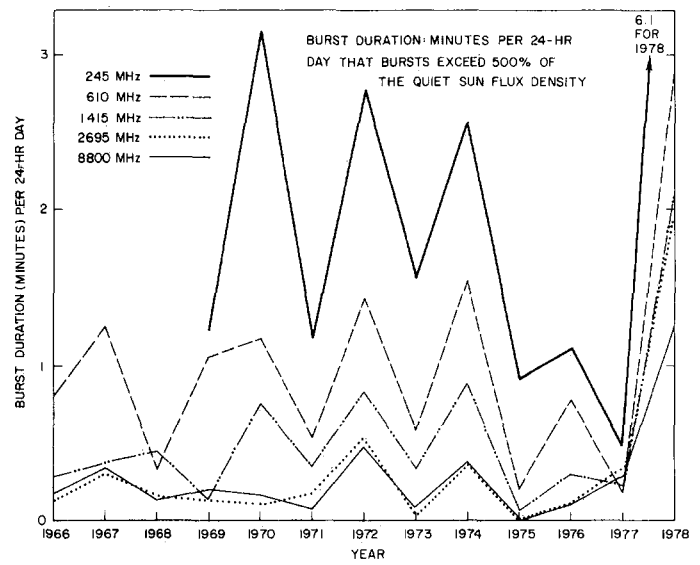


Figure 11-9. The number of minutes per day that solar burst radiation, at various frequencies, exceeded 500% of the quiet-sun flux density.

“outage” times obtained (~ 1 min/day) result from sporadic events during which the burst radiation from the sun may exceed the indicated thresholds for durations ranging from ~10 min to 2 hours.

At the higher radio frequencies (above 500 MHz), strong solar radio interference (above the quiet-sun level) occurs as distinct, individually-identifiable radio bursts. The bursts have different spectral (frequency) characteristics, but at a given frequency the burst has a start time, a peak (or several peaks), and a time of decay. At lower frequencies (245

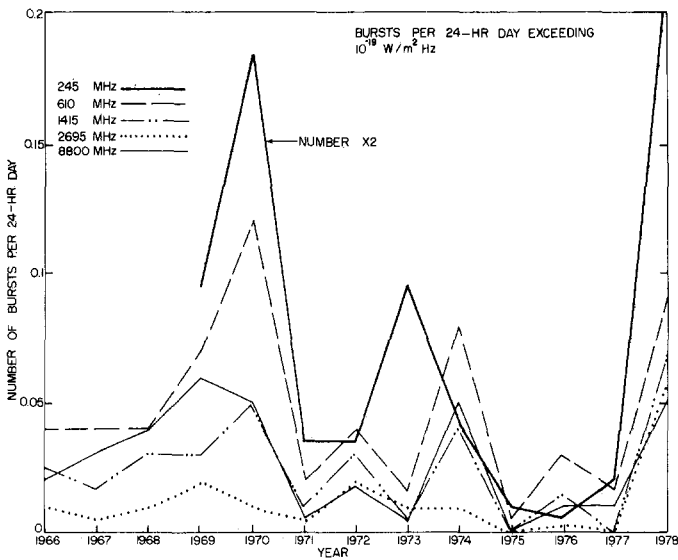


Figure 11-8. The number of bursts during a 24-hr day that exceeded, at various frequencies, 1000 sfu.

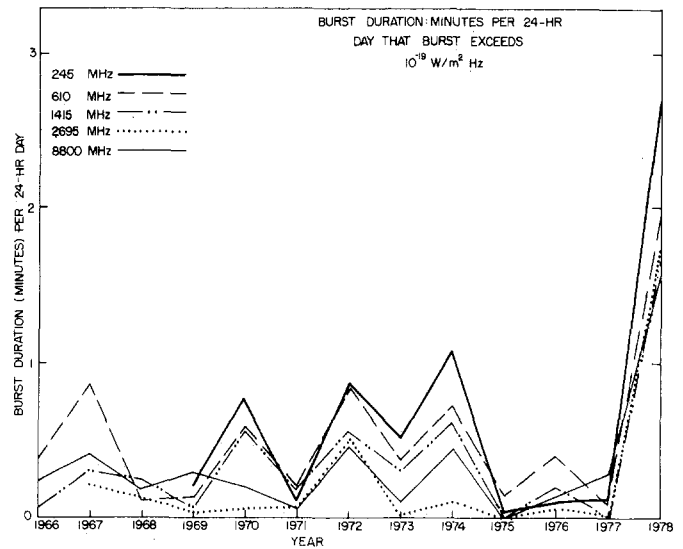


Figure 11-10. The number of minutes per day that solar-burst radiation, at various frequencies, exceeded 1000 sfu.

CHAPTER 11

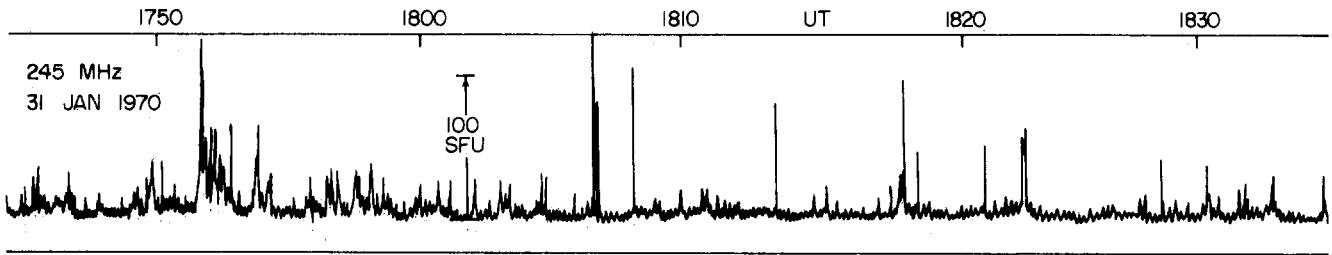


Figure 11-11. The time-intensity profile of a typical 245 MHz noise storm observed at Sagamore Hill.

MHz, for example) there is, in addition to distinct radio bursts, another phenomenon known as solar noise storms. These storms, more prevalent during the sunspot-maximum portion of the 11-year cycle, often last for many hours and sometimes last for a period of days. The noise storms consist of very irregular low-to-moderate increases in solar flux density above the quiet-sun level. For only a very small portion of the noise storm's duration does the added flux density exceed the moderate level (for example, 100 sfu). Figure 11-11 shows a typical example of such a noise storm observed at 245 MHz.

Since these noise storms constitute another significant type of solar radio interference for systems with operating frequencies below 500 MHz, we have also included a statistical graph on noise storm duration, based on our 245 MHz data. See Figure 11-12. The statistical duration is given in terms of minutes of noise storm occurrence per 24-hr day. The shortened period plotted (only 1970 to 1978) gives some indication of the sunspot-cycle variation.

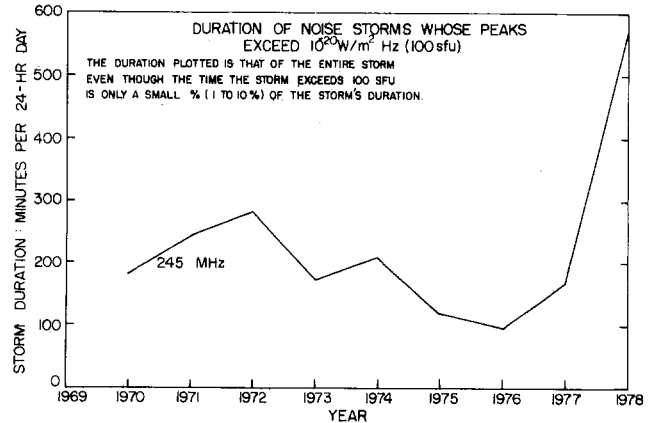


Figure 11-12. The average number of minutes per 24-hr day that a noise storm was reported by Sagamore Hill observatory for the years 1970–1978. The large peak in 1978 may be due (at least partially) to a change in reporting procedures.

REFERENCES

- Barron, W.R., E.W. Cliver, D.A. Guidice, and V.L. Badillo, "An Atlas of Selected Multi-Frequency Radio Bursts from the Twentieth Solar Cycle," AFGL-TR-80-0098 ADA088220 1980.
- Castelli, J.P., J. Aarons, D.A. Guidice, and R.M. Straka, "The Solar Radio Patrol Network of the USAF and its Application," *Proc. IEEE*, **61**: 1307, 1973.
- Forbes, J.M. and R.M. Straka, "Correlation Between Exospheric Temperature and Various Indicators of Solar Activity," AFCRL-TR-73-0378, AD766421 1973.
- Kruger, A., *Introduction to Solar Radio Astronomy and Radio Phys.*, D. Reidel, Dordrecht, Holland, 1979.
- Kundu, M.R., *Solar Radio Astronomy*, Interscience, New York, 1965.
- Kundu, M.R. and T.E. Gergely (eds.), *Radio Physics of the Sun*, IAU Symp. No. 86, D. Reidel, Dordrecht, Holland, 1980.
- Kundu, M.R. and L. Vlahos, "Solar Microwave Bursts—A Review," *Space Sci. Rev.*, **32**: 405, 1982.
- Tanaka, H., J.P. Castelli, A.E. Covington, A. Kruger, R.L. Landecker, and A. Tlamicha, "Absolute Calibration of Solar Radio Flux Density in the Microwave Region," *Solar Phys.*, **29**: 243, 1973.
- Zheleznyakov, V.V., *Radio Emission of the Sun and Planets* (in Russ.) Izdat. 'Nauka', Moscow 1964 Engl. Transl. Pergamon Press, 1970.